Article

Journal of
Nanoscience and Nanotechnology
Vol. 17, 1592–1600, 2017
www.aspbs.com/jnn

Study of the Performances of a Thermoelectric Generator Based on a Catalytic Meso-Scale H_2/C_3H_8 Fueled Combustor

Hossein Abedi[1,*], Laura Merotto[2], Carlo Fanciulli[1], Roberto Dondè[2], Silvana De Iuliis[2], and Francesca Passaretti[1]

[1] *Consiglio Nazionale Delle Ricerche – Istituto di Chimica Della Materia Condensata e di Tecnologie per l'Energia, Corso Promessi Sposi 29, 23900, Lecco, Italy*
[2] *Consiglio Nazionale Delle Ricerche – Istituto di Chimica Della Materia Condensata e di Tecnologie per l'Energia, Via Cozzi 53, 20125 Milano, Italy*

In this work the thermoelectric generator (TEG) based on catalytic combustion already developed in our lab has been further investigated and improved. The system made of two thermoelectric (TE) modules coupled with a catalytic combustor has been used in this work to obtain higher overall efficiency by adding hydrogen to the fuel mixture. Since implementation of hydrogen as a fuel has shown low and stable combustion temperature in literature, it is expected to achieve good overall efficiency of TEG. Moreover, hydrogen can be used to improve the system inducing self-ignition. Focus of the present work is the implementation of different mixture proportions, varying the amount of hydrogen, and the investigation of their effects on the overall efficiency. The overall TEG efficiency, has been evaluated by parallel characterization of thermoelectric modules and exhaust gases composition. The system performances have been characterized using different mixtures: the results indicate that addition of H_2 to the fuel contribute to increase the chemical and overall TEG efficiency respect to previous work, producing up to 5.92 W of electrical power. Finally, the effects of H_2 for on self-ignition conditions have been investigated finding the minimum H_2 amount for different gas flow rates.

Keywords: Thermo-Electric Generator, Portable Energy Production, Meso-Scale Catalytic Combustor, Hydrogen-Propane Catalytic Combustion, Self-Ignition.

1. INTRODUCTION

The miniaturization of mechanical and electromechanical engineering devices has received growing attention in recent years. This is due to the increasing interest in innovative solutions for microelectronics, biomechanics, molecular biology, and microfabrication techniques.[2] The advances in miniaturized mechanical devices open interesting new opportunities for combustion, especially in the field of micro power generation,[3,4] allowing the development of power-supply devices having high specific energy (small size, low weight, long duration).[5,6] Due to their small scale, effects of flame-wall interaction and molecular diffusion are more significant in micro and meso-scale combustion[3,5] when compared to larger combustion systems. These effects are still not completely understood and require further investigation.

Hydrocarbon-based devices as portable power sources are a suitable alternative to common batteries[7–10] because of their high energy density. These fuels can be used both in homogeneous combustion[11–17] and catalytic reactors.[18–23]

The major drawback of conventional homogeneous (gas-phase) combustion systems lies in the very high (>1500 °C) operating temperatures, which results in a significant limitation of material selection and in the need of extensive combustor insulation. Further strong limitations of these devices are strictly related to their dimensions. As the size decreases, the surface area-to-volume ratio of the combustor increases with a subsequent increase of the heat-loss to heat-generation ratio. These strong losses in the small dimension induce flame quenching,[2–4] and are also responsible for an increase in pollutants emission such as CO and unburned hydrocarbons. In addition, the smaller the volume, the shorter the flow residence time.

*Author to whom correspondence should be addressed.

 1533-4880/2017/17/1592/009 doi:10.1166/jnn.2017.13731

In order to overcome the aforementioned limits, a suitable solution for small devices is catalytic combustion.[24, 25] When implemented in micro/meso scale devices, catalytic combustion allows full utilization of the hydrocarbon fuels high energy densities, but at notably lower operating temperatures than those typical of traditional combustion. Additionally, catalytic systems are generally easier to start, more robust to heat losses, and self-sustained at leaner fuel/air ratios.[26–29]

Compared to fuel cells or other combustion-based systems, thermoelectric (TE) power generators are attractive for portable systems due to their compactness, reliability and high power densities. Considering the present commercial bismuth telluride-based TE modules, the operating hot temperature limit in continuous regime is generally close to 300 °C, which is too low to be compatible with the temperatures of a standard combustor. Therefore, catalytic combustion is particularly well suited for TE power generation because of this relatively low temperature ceiling.

There are many examples of micro- and mesoscale thermoelectric power generators powered by catalytic combustion in available literature.[30–34] A TE generator fabricated from silicon bonded to glass developed by Yoshida et al.[34] was able to produce 184 mW of electrical power with an efficiency of 2.8% from the catalytic combustion of hydrogen. Norton and co-workers[6] reported for their integrated combustor-TE generator the production of 1 W maximum power and a thermal-to-electrical conversion efficiency of 1.08% with hydrogen as the fuel. The group has also reported the generation of 0.45 W electrical power with propane as the fuel at 0.42% conversion efficiency, using propane lower heating value LHV.[35] In recent years, Marton and co-workers[36] developed a butane-fueled thermoelectric generator (TEG) delivering 5.82 W maximum power with 2.53% conversion efficiency. Several efforts have been made by different authors to investigate the hot gases recirculation in order to reduce heat losses and thus increase the efficiency of this kind of systems.[37–39] Nevertheless, the demonstration of a fuel-based TEG suitable for portable power with energy density comparable to that of a battery remains an open challenge.

In this work, a thermoelectric generator (TEG) based on a catalytic meso-scale combustor coupled with commercial thermoelectric modules fueled with propane and hydrogen is investigated in terms of electric power obtained and thermal to electric conversion efficiency. The combustor is used as heat source in a sandwich between two TE modules, in order to achieve an electrical power output having I–V characteristics suitable for supplying small electrical devices.

The meso-scale combustor used in this work is designed with the aim to exploit the platinum catalytic effect on hydrocarbon fuel combustion and to be efficiently coupled with commercial TE modules, as described in Ref. [1]. Chemical efficiency was estimated analyzing the exhaust gases concentration with Fourier transform infrared spectroscopy (FT-IR), which allows a quantitative estimation of the gases composition at the combustor exhaust.[31, 39]

The meso-combustor developed in Ref. [1] has shown significant advantages when compared to similar solutions presented in the literature.[6–8] The first advantage is the use of a low-cost, commercially available catalyst, with no need for *ad hoc* manufacturing allowing to obtain the desired wall temperatures for thermoelectric modules coupling with no need for intermediate heat dissipation, thus resulting in smaller fuel consumption and a more compact design. The commercial TE modules used are not specifically designed for power applications, but the refined thermal control of the combustor allowed to reach performances representing an improvement in portable-scale electrical power converters based on thermoelectric technology and hydrocarbon fuels. Following these results, the same system has been used in this work to obtain higher overall efficiency by adding hydrogen to the fuel mixture. Since implementation of hydrogen as a fuel has shown low and stable combustion temperature in literature,[40] it is expected to achieve good overall efficiency of TEG. Focus of the present work is the implementation of different mixtures, varying the amount of hydrogen, and the investigation of their effects on the system overall efficiency.

Characterization of thermoelectric modules and exhaust gases concentration are simultaneously performed in order to evaluate the overall TEG efficiency. Furthermore, the system obtained has been characterized in different operating conditions measuring the delivered electric power. The results are compared to the ones already reported in order to evaluate the effects of the new mixture on the system performances.

2. MATERIALS AND METHODS

A thermoelectric generator (TEG) was designed coupling a catalytic premixed meso-scale combustor and thermoelectric commercial modules.

The sketch of the TEG developed is reported in Figure 1. Here, two thermoelectric (TE) modules are placed in a thermal chain consisting of the catalytic combustor surfaces (hot side) and two water-cooled heat sinks (cold side). In order to provide the most efficient contact at the interfaces between the TE modules with

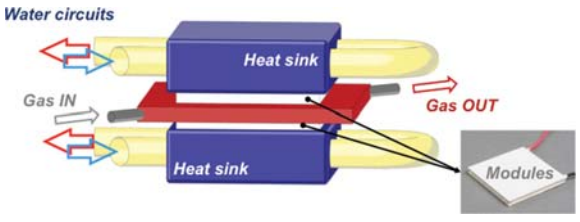

Figure 1. Sketch of the thermoelectric generator obtained by coupling the combustor with two commercial thermoelectric modules.

the combustor surface and the heat sink, graphite sheets (100 μm thick) are used. Graphite was chosen for its capability for compensating the effects of surface roughness and was preferred to thermal pastes for its high reproducibility and stability. The heat sinks are aluminium bulks homogeneously cooled by a 13 °C water flowing in the circuit at 2.5 l/min volume rate. The cooling system is arranged in order to provide similar thermal conditions at both TEG sides. To ensure the thermal chain, the system is held together by two metal springs and four bolds and nuts. The compressive system allows obtaining a homogeneous pressure on the surfaces, minimizing thermal losses, compensating the increase of pressure on the TE modules due to the thermal expansion, and preserving the thermal chain components correct alignment. The compressive system is set to press the column with 0.5 MPa: this value is at the lower limit suggested for modules usage. The choice has been determined considering the effects of the pressure on the overall chain. In fact, the combustion chamber corresponds to the module shape and it is closed by a thin steel layer. An excess of pressure could cause, with the temperature, a loss in planarity of the system reducing the coupling with the modules.

In this work, 40×40 mm^2 Ferrotec commercial modules for cooling, based on chalcogenides, are used. Each module have 126 couples with square elements of 1.5×1.5 mm^2. Tests performed on the devices allowed to identifying a maximum temperature at the hot side equal to 256 °C due to the soldering materials used for the assembly of the thermocouples. These modules are designed for cooling applications, so no data for power generation are available. However, each module has been tested in order to define the conversion capability of the device, obtaining a response in terms of Seebeck value of 35 mV/K averaged on the temperature range between 5 °C and 98 °C. The internal resistance of the modules, useful for maximum power at the matching load calculation, is about 4 Ω. The power output is a function both of the load and of the ΔT applied to the module: using a $\Delta T = 140$ °C, the maximum power produced by a single module is in the order of 2.0 W corresponding to a V–I couple of 2.9 V and 0.6 A, respectively.

In Figure 2 a sketch of the meso-scale combustor is shown. The geometry used for the combustion chamber was chosen in order to match the size of the TE devices. The aluminum-made combustor is a $40 \times 40 \times 4$ mm^3 chamber filled with 155 commercial alumina cylindrical pellets ($r = 1.6$ mm, $h = 3.2$ mm) covered with a thin catalytic film (platinum 1% weight).

The pellets are placed in ordered lines so that the height of the channel for gas flowing is 0.8 mm. Propane, hydrogen and air are used as fuels and oxidizer, and related flow rates are measured and controlled by using thermal flow meters (Bronkhorst El-Flow F-201CV).

In Table I the fuel mixtures in terms of hydrogen percentage with respect to propane and to the total fuel

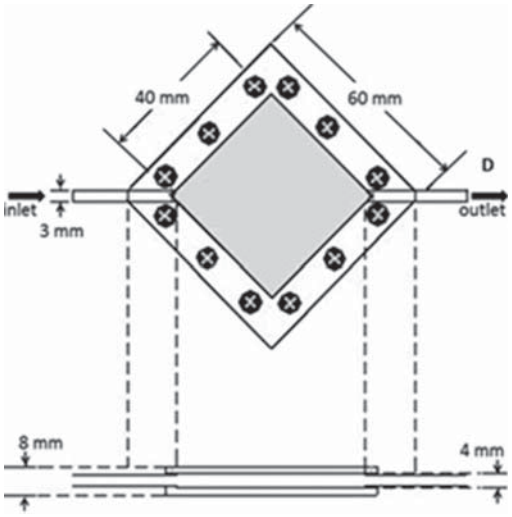

Figure 2. Sketch of the meso-scale combustor used in this work.

amount are reported. The equivalence ratio Φ is set to 1 in the case of C_3H_8/air or H_2/air mixture. In the case of C_3H_8/H_2/air, where three reactants are involved, the second equivalence ratio $\varnothing_F$ defined in Ref. [41] is used and set equal to 1, while keeping the total flow rate constant.

Temperature measurements were carried out using *K*-type thermocouples placed on the combustor surface close to (1 mm) the TE modules as hot side temperature for the top and bottom modules. A *K*-type thermocouple is inserted in the heat sink till 0.5 mm to the surface of the top TE module in order to acquire the cold side temperature. It is assumed that the cold side temperature at the bottom TE Module is equal to the top one. This is reasonable because being the input water the same for both modules, uniform heat removal for the both cold sides is assured.

The accuracy in point measurements is about ±2 °C in the temperature range considered (from −20 °C to +350 °C).

The overall chemical efficiency was estimated by means of Fourier transform infrared spectrometry (FT-IR) analysis of the exhaust gases. The exhaust gases were properly collected from the combustor outlet and sent through a cut-off particulate filter and a water trap to a Thermo

Table I. List of the fuel mixtures under analysis.

	H_2% (respect to)	
Fuel	C_3H_8 [Nl/min]	Total fuel [Nl/min]
C_3H_8	0	0
25% H_2	25	20
50% H_2	50	33.3
75% H_2	75	42.8
100% H_2	100	50
Only H_2	–	100

Scientific Nicolet 6700 FT-IR spectrometer equipped with a variable-pathlength heated gas-cell (Gemini Mars series 6.4 M, internal volume of 0.75 l) positioned inside the instrument. In order to prevent possible carbon residuals condensation, both the transfer line and the gas-cell were maintained at 393 K. The FT-IR spectra are collected with a resolution of 0.5 cm^{-1} and corrected from background.

Quantitative analyses of the gas concentrations were performed by using a previous calibration procedure. The chemical efficiency, η_c, has been calculated using the following relationship:

$$\eta_c = \frac{[CO_2]}{[CO_2]+[CO]+[UHC]}$$

Where [UHC] is the concentration of the total unburned hydrocarbons. The chemical efficiency has been evaluated with TEG system working at its matching load (maximum power production) status. In this condition, in fact, obtained more realistic chemical efficiency can be obtained.

The combustor and the TEG performances were simultaneously characterized at various operating conditions corresponding to different H_2 percentages in the fuel mixtures. The total gas flow rates ranged between 2 Nl/min to 4 Nl/min. The case of C_3H_8/air pure mixture was acknowledged to be used as reference for the following experiments adding H_2. Normal litres per minute (Nl/min) were chosen instead of Kg/s as unit for the gas flow rates in order to homogenize the experimental conditions and be able to directly compare the results changing the fuel mixture composition. In fact, considering 1 Nl/min, C_3H_8/air or H_2/air in stoichiometric condition correspond to 2.12×10^{-5} kg/s and 1.50×10^{-5} kg/s, respectively. Since a premixed fuel/air approached is used to feed the combustor, flow rates are calculated based on normal condition.

The change of the total flow rate allows the characterization at different ΔT of the TEG: being the cold side temperature almost constant due to the power removed by the water cooled circuit, an increase of the hot side temperature is obtained.

The TEG electrical output was studied in terms of voltage and power produced for each ΔT applied. The I–V and I–P characteristics were measured at thermally steady conditions by connecting the TEG output to external loads having increasing values from short-circuit up to open-circuit.

The data obtained from combustor and TEG characterization allowed calculating the electrical conversion efficiency for each module and for the overall device.

3. RESULTS AND DISCUSSION

3.1. Propane/Air Mixtures and Hydrogen/Air Mixtures

The overall system was characterized starting from the two limit cases for the fuel mixtures: 100% C_3H_8 and 100% H_2. In Figure 3 electrical outputs are reported for each module and for the in-series configuration. In particular, power versus current (a, c) and voltage versus current (b, d) are shown for propane and hydrogen, respectively. Comparing the two fuel conditions, similar trends are obtained for both power and voltage values: this is related to the similar ΔT values set by changing the total fuel flow rate. In this case, looking for a direct comparison between the two fuels, the same values at the hot side temperature have been imposed, equal to 168 °C for hydrogen and 163 °C for propane. These values have been obtained with a low difference in total gas flow rates for the two fuels, 2.8 Nl/min (4.2×10^{-5} kg/s) for hydrogen/air and 3 Nl/min (6.3×10^{-5} kg/s) for propane/air, displaying a slightly higher efficiency of H_2 combustion. As a further interesting observation, a difference in the temperature distribution is observed: the hotter side of the combustor appears to be the top one for H_2 fuel and the bottom one for C_3H_8. This effect could be related to the different densities of the two gases which is responsible of a positioning of the combustion in the upper volume of the chamber for hydrogen and in the lower for propane. Figure 3 displays that ΔT is larger at the top side in all the cases, in contrast with the T_h measurements, but this can be explained with the natural heat flow in the experimental setup. However, the comparison between the two V_{oc} values (top and bottom) in the cases of C_3H_8 and H_2 mixtures shows how the discrepancy is approximatively null in the former case, while in the latter it is larger due not to an enhancement of the top result but to the reduction of the bottom one.

3.2. Propane/Hydrogen Mixture Fuels

3.2.1. TE Conversion Efficiency

The performances of the TEG modules are investigated by increasing H_2 content in the fuel. To this purpose, thermoelectric conversion parameters are evaluated by changing the experimental conditions. In Figures 4 and 5 efficiency and maximum power respectively are reported as a function of H_2 content in the fuel for several total flow rates. In the plots, 0% refers to the case of only propane analyses, while the values corresponding to only hydrogen are reported at the end of the x-axis.

As it can be seen in Figure 4, by increasing H_2 fraction in the fuel, an improvement of TE conversion efficiency is obtained. In all cases the efficiency mildly increases up to 50% H_2 and slightly decreases above this value. In the 4 Nl/min case, the increase in conversion efficiency is less significant, as the system is already working close to the maximum efficiency reported.[1] This rate also represents the TEG system operation limit due to the value of T_h reached by the combustor. It is worth noticing that the conversion efficiency obtained by the coupled system is not equal to the duplication of the best single module efficiency. The measured conversion efficiency in the best case (4 Nl/min, 50% H_2, 8.4×10^{-5} kg/s) for the overall TEG

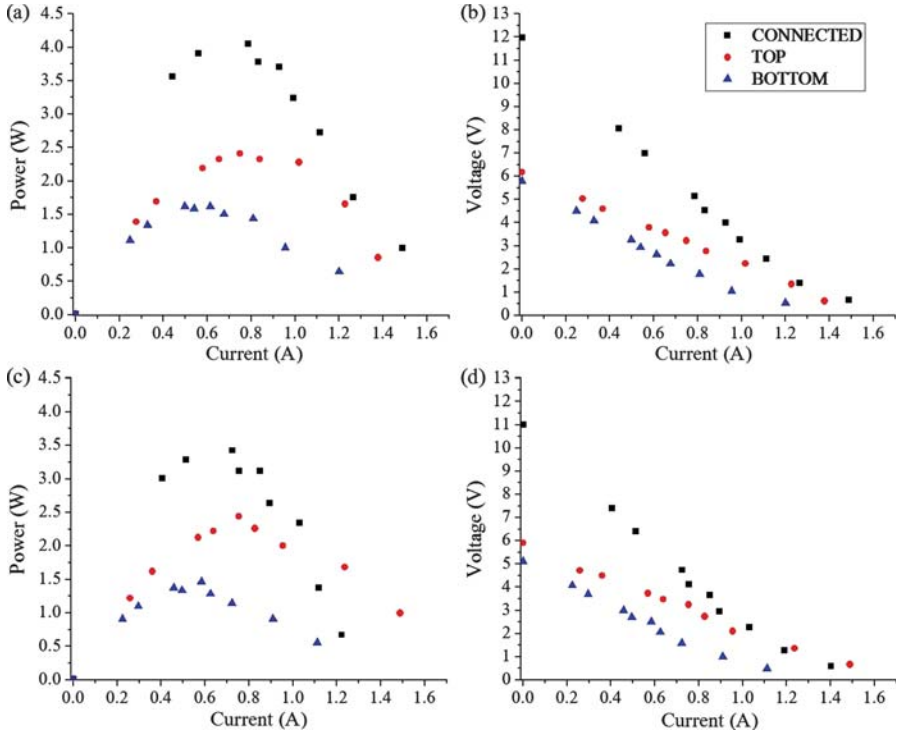

Figure 3. TE Module electrical output curves. (a) Power versus current and (b) voltage versus current for propane, with 3 Nl/min (6.3×10^{-5} kg/s) T_h top: 158 °C T_h bottom: 163 °C, (c) power versus current and (d) voltage versus current for hydrogen, with 2.8 Nl/min (4.2×10^{-5} kg/s), T_h top: 168 °C T_h bottom: 153 °C.

system is 2.35, while a value close to 2.8 would be reached doubling the best single module efficiency. The reason for such discrepancy can be found in the fact that the two modules connected in series are not at the same temperature difference leading to reduced performances according to Ref. [42].

Although TE conversion efficiency using only H_2 is close to the case of best efficiency for the same total flow rates, the system results to be less stable.

The overall maximum power delivered versus hydrogen content is shown in Figure 5. A continuous increase in electrical power delivered is detected by adding H_2 to the mixture. A similar behavior has been observed for the voltage output. The power produced for the TEG system for 4 Nl/min total flow rate and 50% H_2 is 5.92 W.

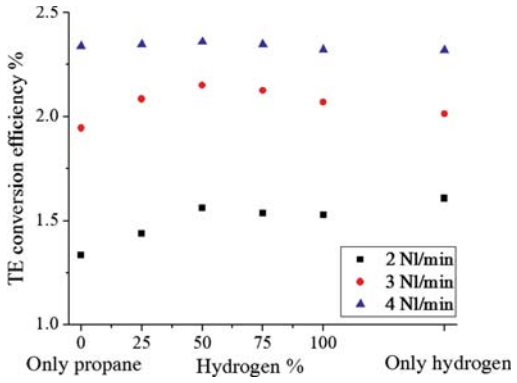

Figure 4. TE Module conversion efficiency versus hydrogen content for 2, 3 and 4 Nl/min total flow rates having Φ and $\varnothing_F$ equal to 1, TE modules at the maximum power state (TE modules are attached with 6.6 Ω resistance equal to their internal resistances).

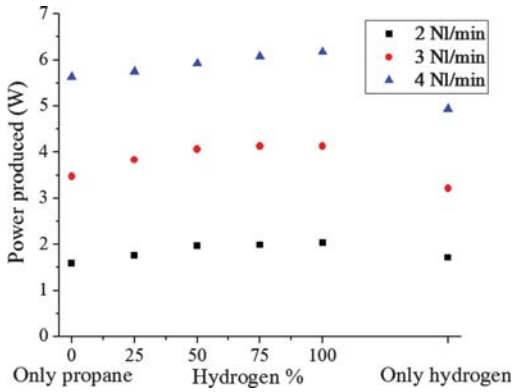

Figure 5. Overall power produced versus hydrogen content, the maximum power is calculated at 6.6 Ω which is the internal resistance of TE Modules. (TE modules are connected).

Again, considering the two modules working independently, adding each single module result, the power is 6.30 W. The overall power produced in case of H_2/air is considerably lower than the case of the C_3H_8/H_2/air mixture. Considering the results previously reported,[1] the performances found in this work are close to the one already observed, differing in the range of experimental errors.

3.2.2. Chemical Efficiency

The chemical efficiency is investigated as a function of the fuel composition for different flow rates by measuring the gas composition at the exhaust of the meso-scale device via FT-IR spectroscopy.[1] In Figure 6 unburned propane (a), CO (b), CO_2 (c) and the corresponding chemical efficiency are reported as a function of hydrogen content for the different total flow rate values under analysis.

As it can be seen in these figures, increasing hydrogen content results in a decrease in the unburned C_3H_8 and a corresponding increase of CO_2 concentration. Moreover, CO concentration increases (Fig. 6(d)) with hydrogen content, even if it plays a side role in the chemical efficiency.

From Figure 6(a) it can be seen that H_2 addition to the mixture, at constant total flow rate, results in a significant increase in chemical efficiency. The chemical efficiency increases up to a certain amount of H_2 and then starts to decrease by further adding hydrogen. Growing with the total flow rate, the chemical efficiencies improve and the peak of efficiency shifts to lower H_2 percentages. The 4 Nl/min total flow rate with 50%H_2 shows the highest chemical efficiency (96.4%), the temperature is about 220 °C at the hot side of thermoelectric module (at the open circuit condition) ensuring safety of the TE modules.

3.2.3. Overall TEG Efficiency

Finally, the overall TEG efficiency is evaluated as the product of chemical and TE conversion efficiencies. In Figure 7 this result is reported as a function of the fuel composition for different flow rates. H_2 addition to the fuel mixture results in an overall TEG efficiency increase up to 60% of hydrogen content. The same behavior is observed for all the total flow rates investigated. The efficiency improvement reported for 4 Nl/min varying H_2 is slighter than the one observed for the other cases. This is because the TE conversion efficiency is close to its maximum value as reported in Ref [1]. The maximum value for overall efficiency is 2.27 corresponding to 4 Nl/min with 50% H_2. Considering the mirroring of single module results, the overall efficiency is 2.66.

Summarizing, having 4 Nl/min flow rate mixture of 50% H_2/C_3H_8/air can provide the best power conversion (5.92 W to 6.3 W) for the present TEG system with chemical efficiency (96.4%) and TE conversion efficiency (2.35 to 2.77) leading to an overall efficiency ranging between 2.27 and 2.67. These results indicate that

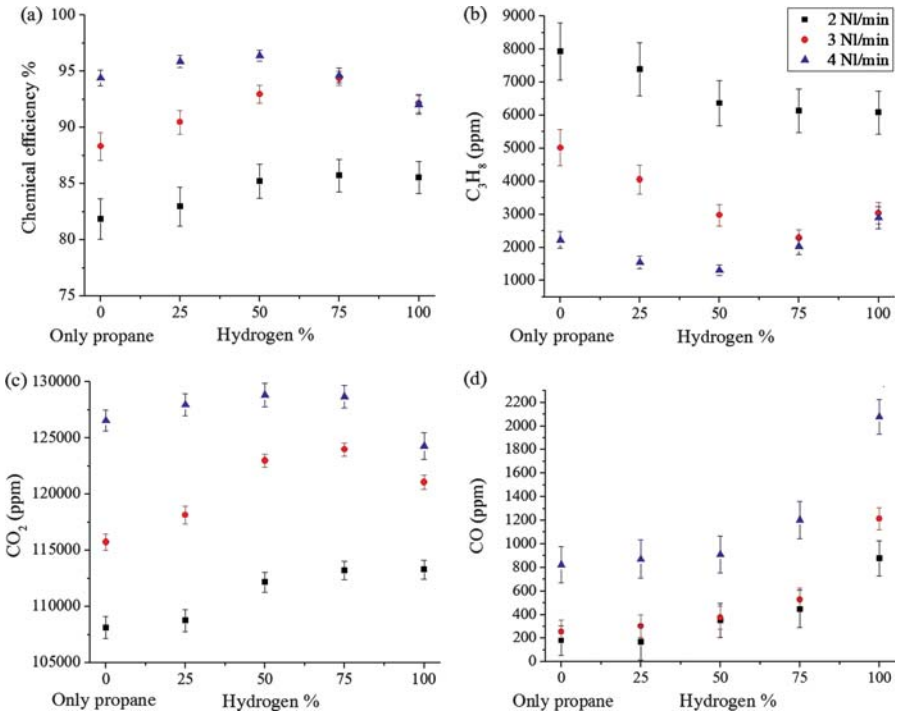

Figure 6. Chemical efficiency results: 2, 3 and 4 Nl/min total flow rates having Φ and $\varnothing_F$ equal to 1, TE modules at the maximum power state (TE modules are attached with 6.6 Ω resistance equal to their internal resistances) (a) chemical efficiency (b) unburnt C_3H_8 concentration (in ppm) (c) CO_2 concentration (in ppm) (d) CO concentration (in ppm) at the exhaust gases.

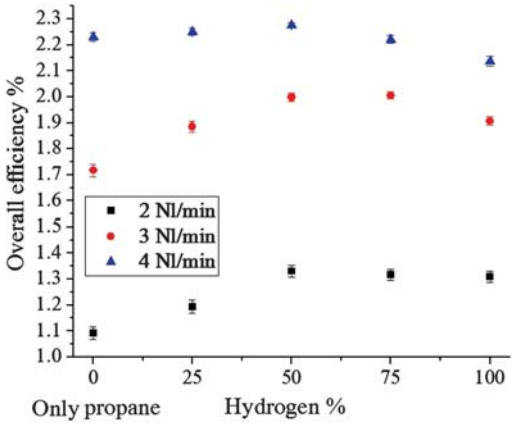

Figure 7. Overall efficiency versus hydrogen content of the system assembled.

addition of H_2 to the fuel results in increased chemical efficiency with respect to the results reported in previous work.

3.3. Self-Ignition Investigation

As C_3H_8/air and some cases of C_3H_8/H_2/air mixture are not self-igniting in contrast with H_2/air mixture, hydrogen assisted ignition is necessary. The occurring of ignition is evaluated by measuring the combustor temperature. At constant fuel/air flow rate, three temperature measurements are performed at intervals of 1 minute. Ignition occurs if the aforementioned temperature readings differ by more than 50 °C as suggested by Ref. [43].

The minimum amount of H_2 required for self-ignition for C_3H_8/H_2/air mixture is investigated in different conditions:

(a) opening C_3H_8, H_2 and air flows simultaneously without water cooling;

(b) opening C_3H_8, H_2 and air flows simultaneously with water cooling;

(c) opening H_2/air and waiting for the temperature equilibrium at the combustor before adding the C_3H_8.

The results for the study on the minimum hydrogen amount required in order to self-ignite the combustion process are presented in Table II. The hydrogen amounts are expressed in terms of percentages respect to propane and to the total fuel.

The H_2 percentages are chosen in order to ensure the repeatability of the ignition. Nevertheless, it can be observed that ignition may in some cases occur with lower H_2 amounts: this can be explained taking into account the effect of variable turbulence conditions in the combustion chamber (not investigated in this work).

The minimum H_2 percentage needed for self-ignition is lower at higher total flow rates. For 4 Nl/min total flow rate the minimum H_2 percentage for self-ignition is around 70% which is close to the best TEG efficiencies.

When C_3H_8, H_2 and air are opened simultaneously (cases a and b) self-ignition occurred at a temperature lower than the equilibrium one. Moreover, self-ignition occurs with or without cooling at the TE module cold side in some cases (for 2, 3, 4 Nl/min with 95%, 80%, 75% H_2), while it does not in others (e.g., for 3 Nl/min with 75% H_2). This is believed to be linked to the turbulence in the combustion chamber, rather than to the cooling itself. A higher turbulence results in increased residence time of the gas in the combustion chamber, thus favorably affecting ignition. Moreover, random nature of turbulence is likely to affect the gas mixing in the combustion chamber, thus affecting ignition behavior and leading to possible variations in experiment repetitions.

When H_2/air is opened first (case *c*), the time needed for temperature to reach equilibrium is about 10 minutes. In this case, the equilibrium temperature needed for self-ignition is higher than that measured when C_3H_8, H_2 and air are opened simultaneously. This can be explained taking into account that higher propane total flow rates result in an increased cooling effect in the chamber, preventing self-ignition.

From the results obtained it can be concluded that the ignition depends at least on three important factors: gas temperature, hydrogen amount and turbulence. Therefore, the amount of H_2 needed for self-ignition can be reduced by modifying the combustion chamber design in such a

Table II. Self ignition results: verifying the self-ignition opening $C_3H_8H_2$ and air flow meters simultaneously with/without water cooling or preheating with H_2/air and then adding the C_3H_8.

Total flow rate [Nl/min]	H_2% (respect to) C_3H_8 [Nl/min]	H_2% (respect to) Total fuel [Nl/min]	H_2/air (waiting for T. equilibrium) then adding C_3H_8	H_2/C_3H_8/air simultaneously without cooling	H_2/C_3H_8/air simultaneously with cooling
2	90	47.3	No ignition	Ignition (after 4 min.)	No ignition
2	95	48.7	Ignition (after 3 min.)	Ignition (after 3 min.)	Ignition (after 4 min.)
3	75	42.85	No ignition	No ignition	Ignition (after 2 min.)
3	80	44.4	Ignition (after 3 min.)	Ignition (after 6 min.)	Ignition (after 3 min.)
4	70	41.17	Ignition (after 3 min.)	Ignition (after 3 min.)	No ignition
4	75	42.85	Ignition (after 3 min.)	Ignition (after 3 min.)	Ignition (after 2 min.)

way that the turbulence in the combustion chamber is increased.

4. CONCLUSION

In this work, the combustor developed in a previous paper by the same authors has been characterized changing the fuel mixture. The effects of hydrogen addition to the original propane/air mixture have been investigated in terms of conversion efficiency, power production and electrical characteristics. The efficiency of the system results to be increased by the hydrogen addition up to a 1 to 1 ratio between H_2 and C_3H_8. Increasing the fuel flow rate, the dependence of the overall efficiency on the H_2 content becomes less significant, but in each case going to higher H_2 content leads to a loss in performances. The case of full hydrogen fuel has been checked: a lower flow rate as respect to pure propane is required to produce similar thermal conditions, but high instability of combustion is observed. These results suggest the usage of H_2/C_3H_8 fuel mixture in spite of the pure gases. An investigation of self-ignition conditions has been performed observing that only at high hydrogen contents (above 70%) the system is able to ignite. Residence time and turbulence in the combustion chamber results to be critical parameters for the ignition success. This last investigation is useful to evaluate the possibility to work with the combustor without the need to insert a specific device (like a usual piezoelectric element) for starting the combustion: the fuel composition is not the best performing one, but it still allows good performances and efficiency for the TEG.

Further investigations will be performed in order to study the capability to develop a self-breathing system for the initial fuel mixing with the air, instead to pre-mix them separately before the inlet line. Moreover, dimensioning a passive cooling system will be investigated to assure enough temperature difference and enhance the applicability of TEG system. Moreover, the possibility to use a passive cooling system will be considered to enhance the mobility of the TEG system.

References and Notes

1. L. Merotto, C. Fanciulli, R. Dondè, and S. De Iuliis, *Applied Energy* 162, 346 **(2016)**.
2. J. G. B. F. Vican, B. F. Gajdeczko, F. L. Dryer, D. L. Milius, I. A. Aksay, and R. A. Yetter, *Proceedings of the Combustion Institute* 29, 909 **(2002)**.
3. K. Maruta, *Proceedings of the Combustion Institute* 33, 125 **(2011)**.
4. W. M. Yang, S. K. Chou, C. Shu, H. Xue, Z. W. Li, D. T. Li, and J. F. Pan, *Energy Conversion and Management* 44, 2625 **(2003)**.
5. A. C. Fernandez-Pello, *Proceedings of the Combustion Institute* 29, 883 **(2002)**.
6. D. G. Norton, K. W. Voit, T. Brüggemann, D. G. Vlachos, and E. D. Wetzel, Portable power generation via integrated catalytic microcombustion-thermoelectric devices, *24th Army Science Conference,* Orlando, FL **(2004)**
7. J. Hua, M. Wu, and K. Kumar, *Chemical Engineering Science* 60, 3507 **(2005)**; A. S. Patil, T. G. Dubois, N. Sifer, E. Bostic, K. Gardner, M. Quah, and C. Bolton, *Journal of Power Sources* 136, 220 **(2004)**.
8. S. Yadav, P. Sharma, P. Yamasani, S. Minaev, and S. Kumar, *Applied Physics Letters* 104, 123903 **(2014)**.
9. D. Dunn-Rankin, E. M. Leal, and D. C. Walther, *Progress in Energy and Combustion Science* 31, 422 **(2005)**.
10. W. Choi, S. Kwon, and H. Dong Shin, *International Journal of Hydrogen Energy* 33, 2400 **(2008)**.
11. D. G. Norton, E. D. Wetzel, and D. G. Vlachos, *Industrial and Engineering Chemistry Research* 43, 4833 **(2004)**.
12. T. A. Wierzbicki, I. C. Lee, and A. K. Gupta, *Applied Energy* 130, 350 **(2014)**.
13. A. V. Pattekar and M. V. Kothare, *Journal of Power Sources* 147, 116 **(2005)**.
14. D. G. Norton and D. G. Vlachos, *Combustion and Flame* 138, 97 **(2004)**.
15. N. S. Kaisare and D. G. Vlachos, *Catalysis Today* 120, 96 **(2007)**.
16. C. M. Miesse, R. I. Masel, C. D. Jensen, M. A. Shannon, and M. Short, *AIChE Journal* 50, 3206 **(2004)**.
17. N. S. Kaisare, S. R. Deshmukh, and D. G. Vlachos, *Chemical Engineering Science* 63, 1098 **(2008)**.
18. D. G. Norton, E. D. Wetzel, and D. G. Vlachos, *Industrial and Engineering Chemistry Research* 45, 76 **(2006)**.
19. X. Ouyang, L. Bednarova, R. S. Besser, and P. Ho, *AIChE Journal* 51, 1758 **(2005)**.
20. E. V. Rebrov, M. H. J. M. De Croon, and J. C. Schouten, *Chemical Engineering Research and Design* 81, 744 **(2003)**.
21. S. R. Deshmukh, and D. G. Vlachos, *Combustion and Flame* 149, 366 **(2007)**.
22. G. Saracco, J. W. Veldsink, G. F. Versteeg, and W. P. van Swaaij, *Chemical Engineering Science* 50, 2833 **(1995)**.
23. S. R. Deshmukh, A. B. Mhadeshwar, M. I. Lebedeva, and D. G. Vlachos, *International Journal on Multiscale Computational Engineering* 2, 221 **(2004)**.
24. T. A. Wierzbicki, I. C. Lee, and A. K. Gupta, *Applied Energy* 130, 350 **(2014)**.
25. A. K. Neyestanaki, N. Kumar, and L.-E. Lindfors, *Applied Catalysis B: Environmental* 7.1, 95 **(1995)**.
26. V. Vijayan and A. K. Gupta, *J. Applied Energy* 87, 2628 **(2010)**.
27. V. Vijayan and A. K. Gupta, *J. Applied Energy* 87, 3718 **(2010)**.
28. V. Vijayan and A. K. Gupta, *J. Applied Energy* 88, 2335 **(2011)**.
29. V. Shirsat and A. K. Gupta, *J. Applied Energy* 88, 5069 **(2011)**.
30. P. Aranguren, D. Astrain, A. Rodríguez, and A. Martínez, *Applied Energy* 152, 121 **(2015)**.
31. S. K. Chou, W. M. Yang, K. J. Chua, J. Li, and K. L. Zhang, *Applied Energy* 88.1, 1 **(2011)**.
32. C. E. Kinsella, S. M. O'Shaughnessy, M. J. Deasy, M. Duffy, and A. J. Robinson, *Applied Energy* 114, 80 **(2014)**.
33. H. Xiao, K. Qiu, X. Gou, and Q. Ou, *Applied Energy* 112, 1161 **(2013)**.
34. K. Yoshida, S. Tanaka, S. Tomonari, D. Satoh, and M. Esashi, *Journal of Microelectromechanical Systems* 15, 195 **(2006)**.
35. J. A. Federici, D. G. Norton, T. Bruggeman, and K. W. Voit, *Journal of Power Sources* 161, 1469 **(2006)**.
36. C. H. Marton, G. S. Haldeman, and K. F. Jensen, *Industrial and Engineering Chemistry Research* 50, 8468 **(2011)**.

37. V. Shirsat and A. K. Gupta, *Applied Energy* 88.12, 4294 **(2011)**.
38. E. D. Tolmachoff, W. Allmon, and C. M. Waits, *Applied Energy* 128, 111 **(2014)**.
39. V. Vijayan and A. K. Gupta. *Applied Energy* 87.8, 2628 **(2010)**.
40. S. Allenby, W. C. Chang, A. Megaritis, and M. L. Wyszyński, *Proceedings of the Institution of Mechanical Engineers, Part D: Journal of Automobile Engineering* 215, 405 **(2001)**.
41. G. Yu, C. K. Law, and C. K. Wu, *Combustion and Flame* 63, 339 **(1986)**.
42. A. Montecucco, J. Siviter, and R. A. Knox, *Applied Energy* 123, 47 **(2014)**.
43. Standard Test Method for Thermal Transmission Properties of Thermally Conductive Electrical Insulation Materials, ASTM International, Designation: D5470–12.

Received: 14 March 2016. Accepted: 21 May 2016.